Molecular Crystals and Liquid Crystals

Publication details, including instructions for authors and subscription information:
http://www.tandfonline.com/loi/gmcl20

# Fluctuation Forces Stabilizing Two Kinds of Staircases in Chiral Tilted Fluid Smectics Frustrated between Ferro- and Antiferro-Electricity

Atsuo Fukuda [a b], Hiroyuki Hakoi [a], Miho Sato [a] & Mikhail A. Osipov [c]

[a] Dept. of Kansei Engineering, Shinshu Univ., Ueda, 386-8567, Japan

[b] Dept. of Electronic and Electrical Engineering, Trinity College, Univ. of Dublin, Dublin 2, Ireland

[c] Dept. of Mathematics, Univ. of Strathclyde, Glasgow, G1 1XH, UK

Version of record first published: 18 Oct 2010

To cite this article: Atsuo Fukuda, Hiroyuki Hakoi, Miho Sato & Mikhail A. Osipov (2003): Fluctuation Forces Stabilizing Two Kinds of Staircases in Chiral Tilted Fluid Smectics Frustrated between Ferro- and Antiferro-Electricity, Molecular Crystals and Liquid Crystals, 398:1, 169-187

To link to this article: http://dx.doi.org/10.1080/15421400390221628

*Mol. Cryst. Liq. Cryst.*, Vol. 398, pp. 169–187, 2003

ISSN: 1542-1406 print/1563-5287 online
DOI: 10.1080/15421400390221628



# FLUCTUATION FORCES STABILIZING TWO KINDS OF STAIRCASES IN CHIRAL TILTED FLUID SMECTICS FRUSTRATED BETWEEN FERRO- AND ANTIFERRO-ELECTRICITY

*Atsuo Fukuda*
*Dept. of Kansei Engineering, Shinshu Univ., Ueda 386–8567, Japan*
*Dept. of Electronic and Electrical Engineering, Trinity College, Univ. of Dublin, Dublin 2, Ireland*

*Hiroyuki Hakoi*
*Dept. of Kansei Engineering, Shinshu Univ., Ueda 386–8567, Japan*

*Miho Sato*
*Dept. of Kansei Engineering, Shinshu Univ., Ueda 386–8567, Japan*

*Mikhail A. Osipov*
*Dept. of Mathematics, Univ. of Strathclyde, Glasgow G1 1XH, UK*

*Conventional dispersion and steric interactions between mesogenic molecules generally promote SmC*, while the interlayer orientational correlation between transverse molecular dipoles stabilizes anticlinic $SmC_A^*$. Ferroelectric and antiferroelectric orders thus produced are frustrated because of the X-Y freedom and the low-energy barrier between them. We can naturally explain not only a series of subphases between $SmC_A^*$ and SmC* but also the staircase character of $SmC_\gamma^*$ emerging just below SmA by using the Casimir type long-range interaction due to polarization fluctuations, if we take account of the discrete flexoelectric polarization appropriately in addition to the ordinary one.*

*Keywords*: phase transition; frustrated smectics; subphase; devil's staircase; Casimir force; discrete flexoelectric polarization

One of the authors (AF) thanks Science Foundation Ireland for support based on E. T. S. Walton Fellowship (No. 02/W/I02).

## 1. INTRODUCTION

The synclinc smectic-$C$ phase (Sm$C$) and the anticlinic smectic-$C_A$ phase (Sm$C_A$) are the fundamental mesophases with fluid layers that are observed in the rod-like molecular system. When the constituent molecules make the system chiral, the phases are designated as Sm$C^*$ and Sm$C_A^*$, respectively, and may become ferroelectric and antiferroelectric with spontaneous polarization perpendicular to the tilt plane [1–5]. In many materials, there may exist a sequence of polar subphases with periodical structures of three, four, and more smectic layers between Sm$C_A^*$ and Sm$C^*$ and an additional subphase designated as Sm$C_\alpha^*$ just below Sm$A$ on the high temperature side of Sm$C^*$ — unless Sm$C^*$ is stable, Sm$C_\alpha^*$ and the other subphases may coalesce and emerge between Sm$C_A^*$ and Sm$A$ [5–7]. In the early stage of investigations, Takanishi *et al.* [5,8] and Hiraoka *et al.* [5,9] noticed that Sm$C_\alpha^*$ is not a simple single phase but may constitute a devil's staircase as exemplified in Figure 1. Then, Isozaki *et al.* [5,7] also emphasized that the subphases between Sm$C_A^*$ and Sm$C^*$ must be another devil's staircase. Actual subphase sequences are various and depend, sometimes sensitively, on particular compounds and mixtures as illustrated in Figure 2 [5,10]; the two staircases coalesce as Sm$C^*$ becomes unstable and disappears. It is worth while noticing that racemization makes all the subphases disappear as shown in Figure 3 [5,11]. Sophisticated experimental techniques, such as polarized resonant X-ray scattering [12–14], precision ellipsometry and reflectometry [14–17], advanced polarizing microscopy [18,19] *etc.*, have recently been used to determine the detailed subphase structures. It has unambiguously established that the subphases between Sm$C_A^*$ and Sm$C^*$ with three and four layer periodicities are not coplanar and that the azimuthal angle difference between the directors in adjacent layers is considerably deviated from $\Delta\phi = 0^\circ$ (synclinic) and $180^\circ$ (anticlinic) [14,20]. With respect to Sm$C_\alpha^*$, a short pitch helical structure has recently been emphasized in contrast with the previous suggestion of its devil's staircase, although some successive transitions indicating a staircase character of Sm$C_\alpha^*$ were observed in very thin free-standing films [21].

Two conflicting approaches have been proposed by regarding as important either the continuous short-pitch evolution of the Sm$C_\alpha^*$ helical structure [22–24] or the devil's staircase character not only of subphase emergence between Sm$C_A^*$ and Sm$C^*$ but also of Sm$C_\alpha^*$ itself [25–29]. The first one, called the discrete, clock, or $X$-$Y$ model, takes into account competing orientational interactions between nearest- and next-nearest-neighbor smectic layers by neglecting the entropy effect in the approximation of absolute zero Temperature. Then the minimum of the free energy corresponds to a uniform rotation of the tilt plane about the layer normal,

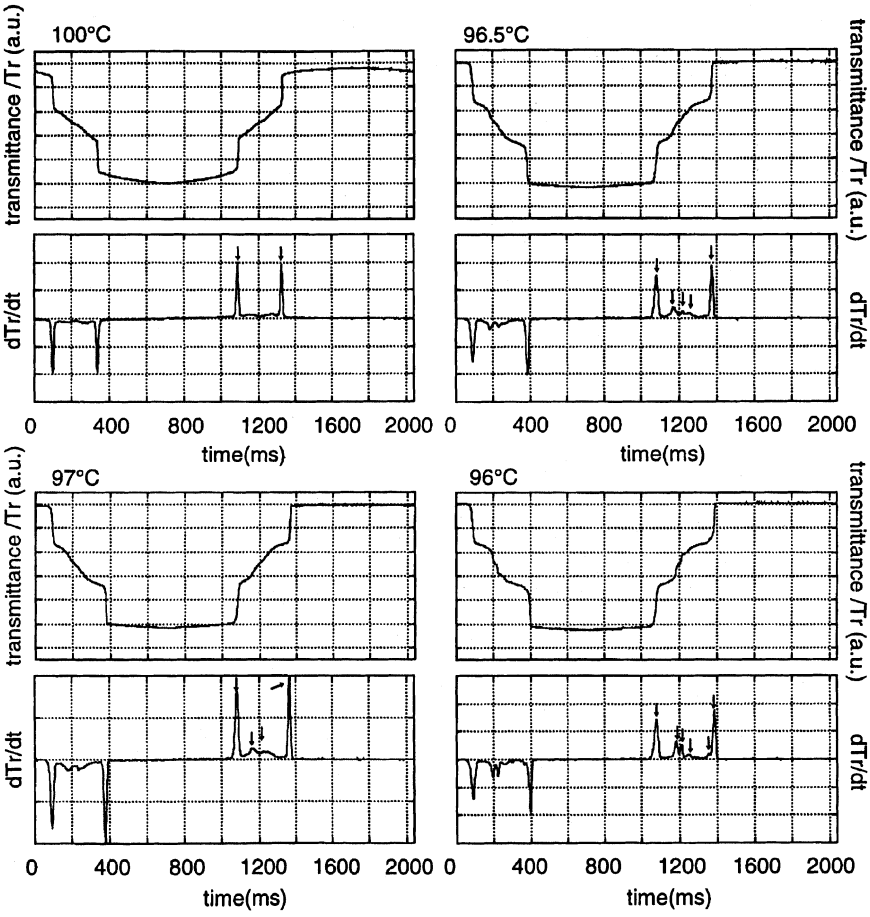


**FIGURE 1** Staircase character of Sm$C^*_\alpha$. Light transmittance under crossed polarizers and electric current were measured at four temperatures within Sm$C^*_\alpha$ by applying a $\pm 60$ $V_{pp}$/6μm triangular wave electric field of 0.5 Hz in a homogeneous cell of MHPOCBC. Note that Sm$C^*_\alpha$ is antiferroelectric at 100°C (upper left) just below Sm$A$, while it is ferrielectric at 96°C (lower right) just above Sm$C^*_A$ [5,8].

and the azimuthal angle difference in adjacent layers is equal to $2\pi q$ where $(1/q)$ is the number of layers in one period. By introducing several much more complicated interactions, we may be able to explain qualitatively the formation of subphases with three and four layer periodicities as well as the continuous short-pitch evolution of Sm$C^*_\alpha$. However, it is difficult to understand naturally the devil's staircase character in Sm$C^*_\alpha$ emerging just below Sm$A$ as well as in a series of subphases between Sm$C^*_A$ and Sm$C^*$.

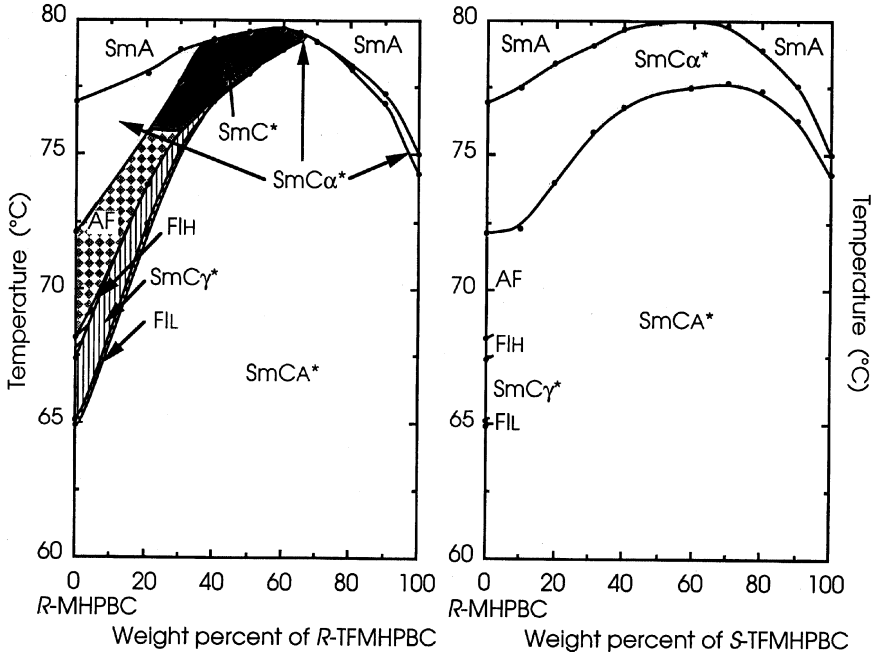


**FIGURE 2** A variety of subphase sequences. Temperature *vs*. mixing ratio ($T$–$x$) phase diagrams were constructed in two mixture systems, (a) ($R$)-MHPBC and ($R$)-TFMHPBC, where the helical pitch grows infinite in between, and (b) ($R$)-MHPBC and ($S$)-TFMHPBC, where the in-layer ordinary spontaneous polarization becomes zero. The subphases with three and four layer periodicities were first designated as Sm$C^*_\gamma$ (ferrielectric) and AF (antiferroelectric but other than Sm$C^*_A$). Later they were also called Sm$C^*_{\mathrm{FI1}}$ and Sm$C^*_{\mathrm{FI2}}$; the designation Sm$C^*_{\mathrm{FI2}}$ is misleading, however, because it is antiferroelectric but not ferrielectric. There exist $\mathrm{FI_L}$ (ferrielectric) and $\mathrm{FI_H}$ (ferrielectric) on the low and high temperature sides of Sm$C^*_\gamma$. Moreover, in other compounds, another subphase FI (ferrielectric) may emerge above AF. Consequently, the most general subphase sequence is 'Sm$C^*_A$-$\mathrm{FI_L}$-Sm$C^*_\gamma$-$\mathrm{FI_H}$-AF-FI-Sm$C^*$-Sm$C^*_\alpha$-SmA', although all of them may not appear at the same time in a particular compound or mixture [5,7].

The second approach is based on the ANNNI (Axial Next Nearest Neighbor Ising) model. It is known that a sequence of subphases which resemble the devil's staircase are indeed obtained in such a model [30,31]. This is a microscopic model and hence the entropy effect, *i.e.* the low orientational order in a smectic layer, plays an essential role. Since the order is as high as 0.7 or more, however, the ANNNI model Hamiltonian can hardly be applied to smectic liquid crystals [32]. In this way, neither of the above models could explain the thus far experimentally observed facts appropriately.

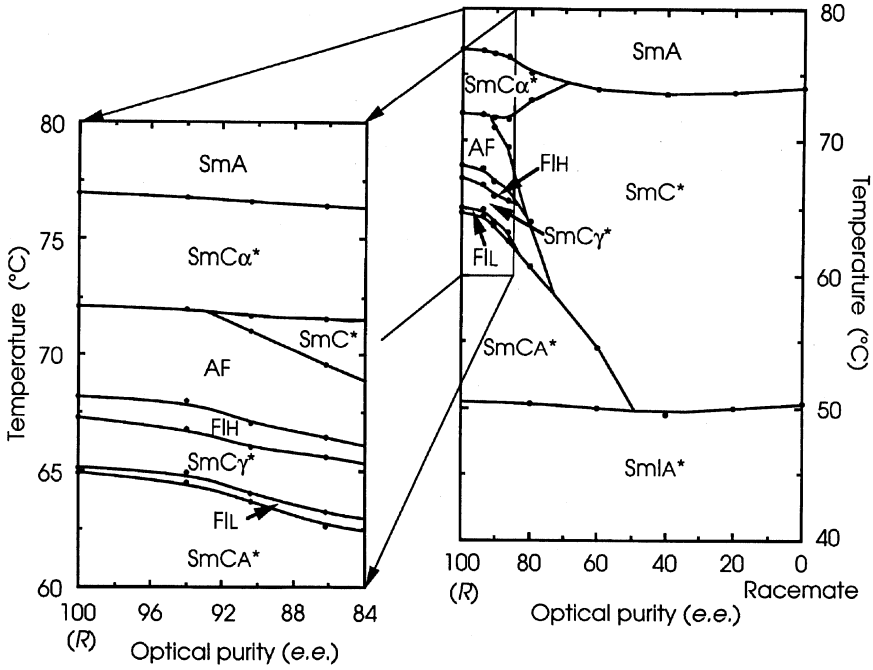


**FIGURE 3** Racemization-induced subphase disappearance. Temperature *vs*. optical purity (enantiomeric excess: *e.e.*) phase diagram was constructed in the mixture system of (*R*)-MHPBC and (*racemate*)-MHPBC. Note that racemization makes all the subphases disappear [5,10].

In solid-state physics, we frequently encounter such large-scale structures as those with periodicities of three, four, and more smectic layers. The presence of some form of frustration is common to the emergence of the structures. At the point in the phase diagram where the dominant ordering forces happen to be equal, a large number of alternative structures may have nearly the same free energy. The frustration may allow us to disclose delicate effects, which otherwise are hard to detect. Two statistical models have been developed which exemplify the emergence of the devil's staircase by lifting the degeneracy [33]. One is ANNNI model described above, and the other is the one-dimensional Ising model with long-range repulsion proposed by Bak and Bruinsma [34,35]. Prost and Bruinsma tried to explain the formation of Sm$C_\alpha^*$ as Well as its devil's staircase character based on the Bak-bruinsma model by taking into account the Casimir type long-range interaction due to polarization fluctuations [36,37]. these polarization fluctuations have been measured and are known to be important for dielectric behavior in SmC* [38]. In the physics of liquid crystals

under consideration, the frustration occurs between ferroelectricity and antiferoelectricity, *i.e.* synclinic Sm$C^*$ and anticlinic Sm$C_A^*$ . In this paper, we first calculate the free energy difference between Sm$C^*$ and Sm$C_A^*$ based on the molecular model developed by Osipov and Fukuda [39], obtaining two frustration points. Then we consider the lifting of degeneracy at these points by the Casimir type long-range interaction due to the polarization fluctuations [36,37]. It will become clear that we have to take account of the discrete flexoelectric polarization, which was introduced to explain the non-planar structures of the subphases [32].



## 2. FREE ENERGY DIFFERENCE BETWEEN Sm$C_A^*$ AND SM$C^*$

Assuming the perfect orientational and translational orders in a system of uniaxial constituent molecules, Osipov and Fukuda have proposed a realistic molecular model for Sm$C_A^*$ [39]. The fundamental phases, synclinic ferroelectric Sm$C^*$ and anticlinic antiferroelectric Sm$C_A^*$, must be stabilized by short-range intermolecular interactions, which are expanded in terms of the spherical invariants. By taking into account only the lowest order non-polar terms, the conventional internal energy as well as the packing entropy resulting from intra-layer interactions is given by

$$U_{eff}^{\perp} = const + (2v_2^{\perp} + v_3^{\perp})\{1 - (\mathbf{n}\cdot\mathbf{e})^2\} + v_4^{\perp}\{1 - (\mathbf{n}\cdot\mathbf{e})^2\}^2. \qquad (1)$$

Here $\mathbf{n}$ is the director in a single layer, $\mathbf{e}$ the layer normal, $v_2^{\perp}, v_3^{\perp}$, and $v_4^{\perp}$ are expansion coefficients. The corresponding free energy normalized by $kT^*$ can be written as

$$\begin{aligned}\frac{F_{\perp}(\Theta)}{kT^*} &= 6(2\tilde{v}_2^{\perp} + \tilde{v}_3^{\perp})\{1 - (\mathbf{n}\cdot e)^2\} + 6\tilde{v}_4^{\perp}\{1 - (\mathbf{n}\cdot e)^2\}^2 \\ &= \alpha(\tilde{T} - 1)\sin^2\Theta + B\sin^4\Theta.\end{aligned} \qquad (2)$$

where $\tilde{v}_2^{\perp} = v_2^{\perp}/kT^*, \tilde{v}_3^{\perp} = v_3^{\perp}/kT^*, \tilde{v}_4^{\perp} = v_4^{\perp}/kT^*$, $\Theta$ is the tilt angle, $\tilde{T} = T/T^*$ the dimensionless temperature normalized by the phase transition temperature between Sm$A$ and Sm$C^*$ or Sm$C_A^*$, and $\alpha > 0$ and $B > 0$ are temperature-independent dimensionless constants. Note that there exist 6 nearest neighbor molecules in the same layer. This is just the Landau type description of the phase transition from Sm$A$ to Sm$C^*$ or Sm$C_A^*$. Hence it would not distinguish Sm$C^*$ and Sm$C_A^*$. The transition temperature and the absolute value of the tilt angle $\Theta$ are mainly determined by Eq. (2). By minimizing Eq. (2) with respect to the tilt angle $\Theta$, we obtain the temperature variation of $\Theta$,

$$\Theta = \frac{180}{\pi}\sin^{-1}\sqrt{\frac{\alpha}{2B}(1 - \tilde{T})}, \qquad (3)$$

which sensitively depends on the parameter ratio $\alpha/B$ as shown in Figure 4.

The free energy resulting from inter-layer interactions are also expanded in terms of the spherical invariants. Taking into account only the lowest order nonpolar terms, *i.e.* the terms which are quadratic in $\mathbf{n}_1$ and $\mathbf{n}_2$, we obtain for the conventional internal energy as well as the packing entropy,

$$U_{eff}^{\parallel} = const + v_1^{\parallel} P_2(\mathbf{n}_1 \cdot \mathbf{n}_2) + v_2^{\parallel}\{(\mathbf{n}_1 \cdot \mathbf{e})^2 + (\mathbf{n}_2 \cdot \mathbf{e})^2\} + v_3^{\parallel}(\mathbf{n}_1 \cdot \mathbf{n}_2)(\mathbf{n}_1 \cdot \mathbf{e})(\mathbf{n}_2 \cdot \mathbf{e}) + v_4^{\parallel}(\mathbf{n}_1 \cdot \mathbf{e})^2(\mathbf{n}_2 \cdot \mathbf{e})^2, \quad (4)$$

and for the transverse dipole orientational correlation,

$$-\frac{1}{2kT}\langle V_{dd}^2(1,2)\rangle_{\mathbf{b}_1,\mathbf{b}_2} = \frac{d_\perp^4}{8kT(L-2l)^6\cos^6\Theta}\{-4-(\mathbf{n}_1\cdot\mathbf{e})^2 + 3(\mathbf{n}_1\cdot\mathbf{e})^2 + 3(\mathbf{n}_2\cdot\mathbf{e})^2 + 6(\mathbf{n}_1\cdot\mathbf{e})(\mathbf{n}_2\cdot\mathbf{e})(\mathbf{n}_1\cdot n_2) - 9(\mathbf{n}_1\cdot\mathbf{e})^2(\mathbf{n}_2\cdot\mathbf{e})^2\}. \quad (5)$$

Here $\mathbf{n}_1$ and $\mathbf{n}_2$ are the directors in adjacent smectic layers, '1' and '2', $\mathbf{e}$ is the smectic layer normal, $d_\perp$ the transverse molecular dipole, $L$ the molecular length, $l$ the distance between the dipole moment in the alkyl

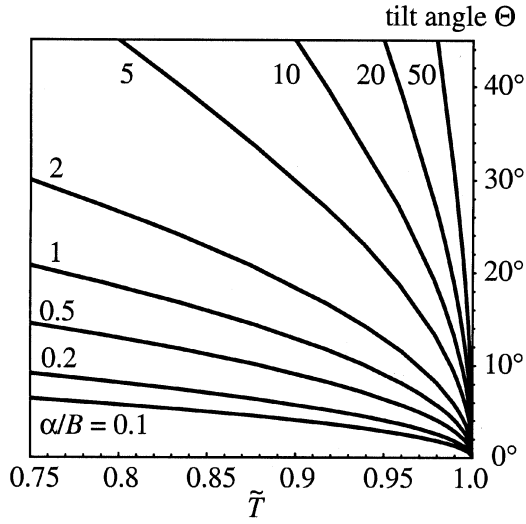


**FIGURE 4** Tilt angle temperature dependence. The phase transition at $T^*$ from Sm$A$ to Sm$C^*$ or Sm$C_A^*$ was described by using the Landau expansion in terms of the normalized temperature $\tilde{T} = T/T^*$ and the dimensionless parameter ratio $\alpha/B$. The tilt angle $\Theta$ (deg.) was calculated as a function of normalized temperature $\tilde{T}$.

chain and the molecular center of mass, and hence $(L - 2l)\cos\Theta$ is the distance between the transverse dipoles of neighboring molecules in adjacent smectic layers. Using Eqs. (4) and (5), we obtain

$$\frac{F_{\parallel}(\phi_1-\phi_2)}{kT^*} = \cos(\phi_1-\phi_2)\sin^2 2\Theta\left(-\frac{1}{2}\tilde{v}_{eff}^{\parallel} + \frac{\tilde{d}_{\perp}^4}{2\tilde{T}\cos^6\Theta}\right) + \cos^2(\phi_1-\phi_2)\sin^4\Theta\left(3\tilde{v}_1^{\parallel} - \frac{\tilde{d}_{\perp}^4}{2\tilde{T}\cos^6\Theta}\right), \quad (6)$$

where $\tilde{d}_{\perp} = d_{\perp}/\{(2kT^*)^{1/2}(L-2l)^{3/2}\}$ is the dimensionless dipole, $\tilde{v}_1^{\parallel} = v_1^{\parallel}/kT^*, \tilde{v}_3^{\parallel} = v_3^{\parallel}/kT^*$, and $\tilde{v}_{eff}^{\parallel} = 3\tilde{v}_1^{\parallel} + \tilde{v}_3^{\parallel}$ are the dimensionless expansion coefficients, and $\phi_1$and $\phi_2$ are the azimuthal angles that specify the orientation of the tilt planes in adjacent layers, '1' and '2'. Note that the number of nearest neighbor molecules in adjacent layers are 2 but only half of it has the head-head position.

In this way, the free energy difference between Sm$C_A^*$ and Sm$C^*$, normalized by $kT^*$ as in Eqs. (2) and (6), can be written

$$\tilde{F}_C - \tilde{F}_{CA} = \frac{F(\phi_1-\phi_2=0^\circ) - F(\phi_1-\phi_2=180^\circ)}{kT^*} = \sin^2 2\Theta\left(-\tilde{v}_{eff}^{\parallel} + \frac{\tilde{d}_{\perp}^4}{\tilde{T}cos^6\Theta}\right). \quad (7)$$

Figure 5 illustrates the phase diagram and the temperature variation of the free energy difference, which are characterized by only two parameters, $\alpha/B$ and $\tilde{d}_{\perp}^4/\tilde{v}_{eff}^{\parallel}$. The ferroelectric and antiferroelectric orders thus produced are frustrated because of the $X$-$Y$ freedom and the low-energy barrier between them. When $\tilde{d}_{\perp}^4/\tilde{v}_{eff}^{\parallel} < 1$, in particular, two frustration points exist: one is the ordinary point where the dominant ordering forces happen to change sign, and the other is slightly peculiar in that three phases, Sm$A$, Sm$C^*$, and Sm$C_A^*$, have the same free energy. The former must be related with a series of subphases between Sm$C_A^*$ and Sm$C^*$, and the latter with the staircase character of Sm$C_{\alpha}^*$. As $\tilde{d}_{\perp}^4/\tilde{v}_{eff}^{\parallel}$ approaches 1, Sm$C^*$ becomes unstable and the two staircases may coalesce.

## 3. THE CASIMIR TYPE LONG-RANGE INTERACTION

Now we consider the degeneracy lifting near the frustration points by the Casimir type long-range interaction due to polarization fluctuations. We begin with the Ising model and specify the subphase structure by $q_T = [F]/([A]+[F])$ in the zero order approximation. Here $[A]$ and $[F]$ are the numbers of anticlinic (antiferroelectric) and synclinic (ferroelectric)

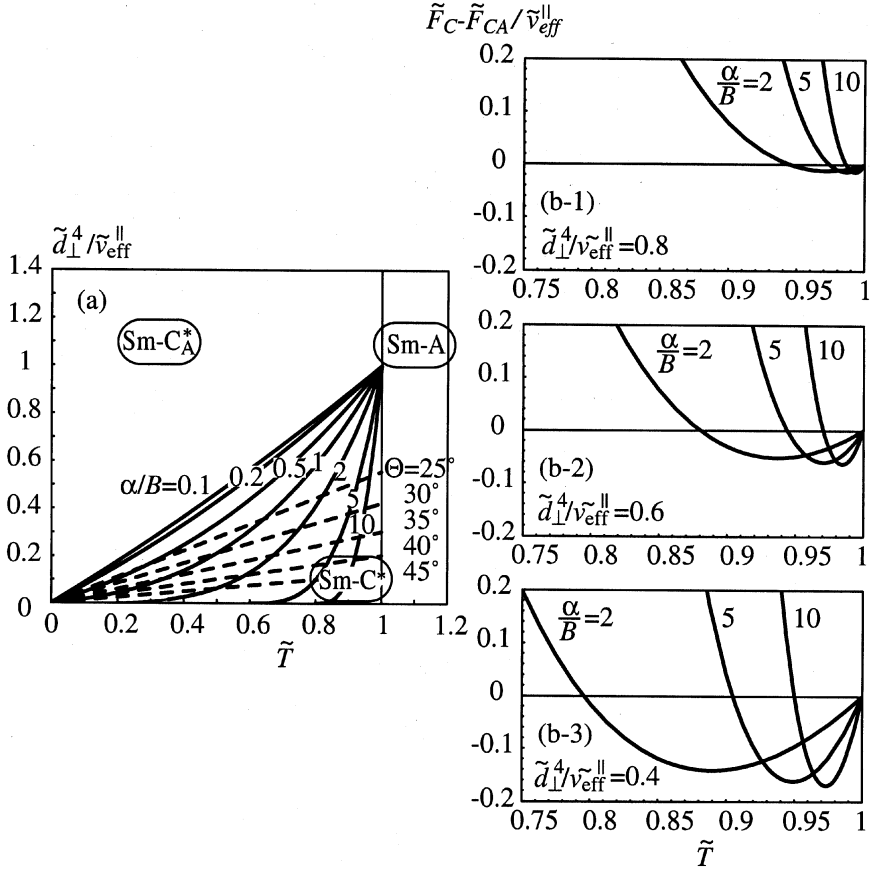


**FIGURE 5** Sm$A$-Sm$C^*$-Sm$C^*_A$ phase diagram and Sm$C^*$-Sm$C^*_A$ free energy difference. (a) A simple phase diagram was calculated in the perfectly ordered smectic liquid crystal which contains Sm$A$, Sm$C^*$, and Sm$C^*_A$. The abscissa is the normalized temperature $\tilde{T}$ and the ordinate is the ratio between dimensionless parameters $\tilde{d}^4_\perp/\tilde{v}^{\parallel}_{eff}$ describing the relative stability of Sm$C^*_A$ and Sm$C^*$. See text for details. The boundary between Sm$C^*_A$ and Sm$C^*$ depends on the tilt angle; solid and dotted lines were obtained by using Eq. (3) and by assuming $\Theta = const$, respectively. (b) The corresponding free energy difference between Sm$C^*_A$ and Sm$C^*$ was calculated as a function of $\tilde{T}$: the parameter $\tilde{d}^4_\perp/\tilde{v}^{\parallel}_{eff}$ was chosen as 0.8 in (b-1), 0.6 in (b-2), and 0.4 in (b-3). The abscissa is $\tilde{T}$ and the ordinate is dimensionless $(\tilde{F}_C - \tilde{F}_{CA})/\tilde{v}^{\parallel}_{eff}$. Note that there exist two frustration points, where the energy difference becomes zero. The chiral interaction was considered only to produce the in-layer spontaneous polarization by disregarding the helical structure. Hence the phase diagram and the free energy difference are the same as those for Sm$A$-Sm$C$-Sm$C_A$ and Sm$C$-Sm$C_A$, respectively [39].

orderings in one period. Note that Yamashita and Miyazima [25] used the $q$ number where $1/q$ is the number of smectic layers contained in a wave (one period). Between $q$ and $q_T$ there is a relation: $q = (1/2)\ (1 - q_T)$. In the following numerical calculations, $q_T$'s used are all the irreducible fractional numbers larger than or equal to 1/10 as well as 0 (Sm$C_A^*$) and 1 (Sm$C^*$). The normalized free energy of a subphase specified by $q_T$ is given by

$$\tilde{\mathcal{F}} = q_T \tilde{F}_C + (1 - q_T)\tilde{F}_{CA} + \frac{1}{kT^*}\left( C \frac{kT}{\sqrt{K_\parallel K_\perp}} \frac{P_0^2}{\varepsilon D} \sum_i \sum_j \frac{S_i S_j}{|i-j|^2} \right). \quad (8)$$

Here $K_\parallel$ and $K_\perp$ are the Frank elastic constants, $D = L\cos\Theta$ is the smectic layer thickness, $\varepsilon$ the dielectric constant, $P_0 S_i$ the dipole-moment per unit area of the $i$th layer along the $y$ axis with the Ising spin $S_i = \pm 1$ [36,37].

Since $P_0 \propto \sin\Theta$, $\sqrt{K_\parallel K_\perp} \propto \sin^2\Theta$, and $\varepsilon$ and $D$ may not sensitively depend on temperature, the Casimir type long-range interaction given by the last term of Eq. (8) can be written as a simplified dimensionless form,

$$\tilde{\mathcal{J}} \tilde{T} \sum_i \sum_j \frac{S_i S_j}{|i-j|^2}, \quad (9)$$

where $\tilde{T} = T/T^*$, and $\tilde{\mathcal{J}} = CP_0^2/(\sqrt{K_\parallel K_\perp}\varepsilon D)$ is a dimensionless temperature-independent constant. Note that the summation depends on a particular subphase structure specified by $q_T$. Regarding the short-range interactions, the $q_T$-dependent part is

$$q_T(\tilde{F}_C - \tilde{F}_{CA}) = q_T \sin^2 2\Theta \left( -\tilde{v}_{eff}^{\parallel} + \frac{\tilde{d}_\perp^4}{\tilde{T}\cos^6\Theta} \right). \quad (10)$$

Consequently, the relative stability of a particular subphase specified by $q_T$ is determined by the $q_T$ - dependent part of Eq. (8),

$$\frac{\tilde{\mathcal{F}}_{qT}}{\tilde{v}_{eff}^{\parallel}} = q_T \sin^2 2\Theta \left( -1 + \frac{1}{\tilde{T}\cos^6\Theta} \frac{\tilde{d}_\perp^4}{\tilde{v}_{eff}^{\parallel}} \right) + \frac{\tilde{\mathcal{J}}}{\tilde{v}_{eff}^{\parallel}} \tilde{T} \sum_i \sum_j \frac{S_i S_j}{|i-j|^2}. \quad (11)$$

We need only three parameters, $\alpha/B$, $\tilde{d}_\perp^4/\tilde{v}_{eff}^{\parallel}$, and $\tilde{\mathcal{J}}/\tilde{v}_{eff}^{\parallel}$. The first one specifies the temperature variation of the tilt angle as given in Eq. (3) and Figure 4. The second describes the relative stability of Sm$C_A^*$ and Sm$C^*$ as seen in Figure 5. The contribution of the Casimir type long-range interaction is determined by the third parameter $\tilde{\mathcal{J}}/\tilde{v}_{eff}^{\parallel}$; when it is negligible, no subphase emerges. Figures 6 (a), (b), and (c) illustrate some numerically calculated results. When $\tilde{\mathcal{J}}/\tilde{v}_{eff}^{\parallel} = 10^{-4}$ and $\tilde{d}_\perp^4/\tilde{v}_{eff}^{\parallel}$ is reasonably smaller than 1, Sm$C^*$ is stable and two staircases emerge on both low and high temperature sides of Sm$C^*$ as a result of degeneracy lifting at the frustration points. As $\tilde{d}_\perp^4/\tilde{v}_{eff}^{\parallel}$ increases, Sm$C^*$ disappears and the two

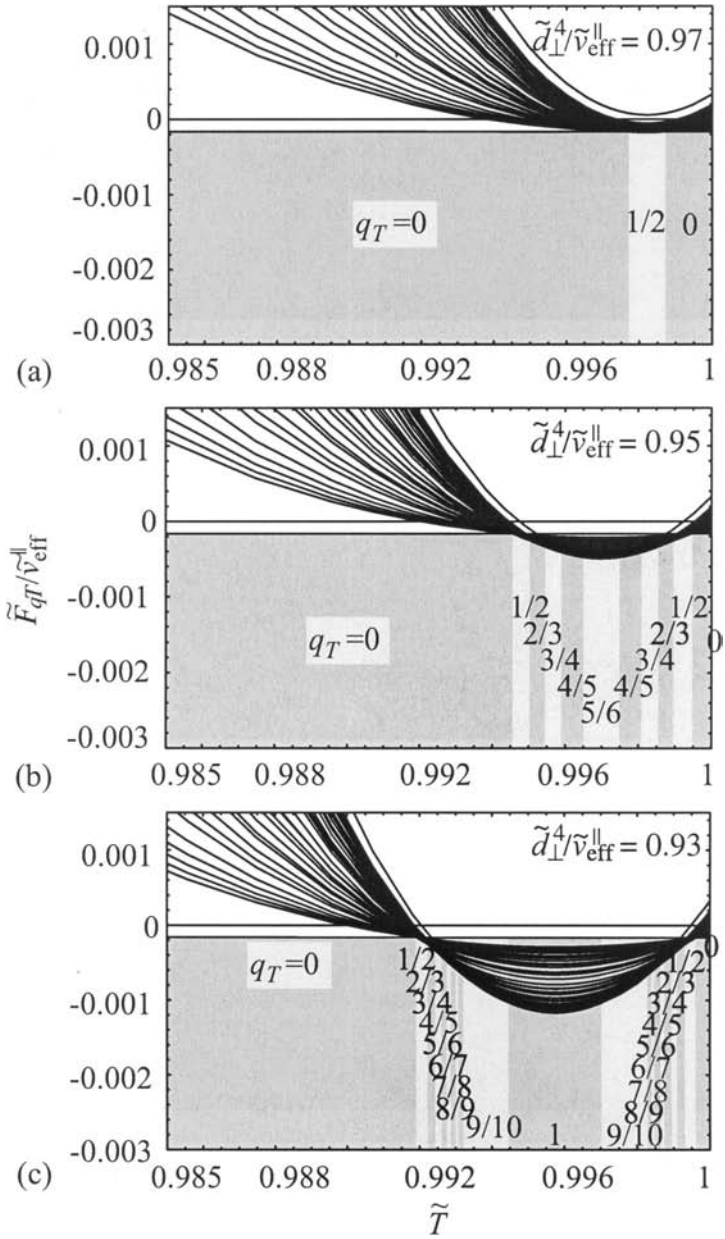


**FIGURE 6** Subphase emergence due to ordinary polarization. The degeneracy lifting near the frustration points was calculated by taking account of the Casimir type long-range interaction due to the ordinary polarization fluctuations. Note that the $q_T = 1/3$ subphase with three layer periodicity ($\mathrm{Sm}C_\gamma^*$), which is experimentally most stable, is never stabilized. Parameters used are $\alpha/B = 5$, and $\tilde{d}_\perp^4/\tilde{v}_{eff}^{\parallel} = 0.97$ in (a), 0.95 in (b), and 0.93 in (c).

staircases coalesce. When $\tilde{d}_{\perp}^{4}/\tilde{v}_{eff}^{\parallel}$ exceeds 1, all subphases disappear and only Sm$C_A^*$ is stabilized.

In this way, the calculated results can explain some aspects of the actually observed subphase sequences in a variety of compounds and mixtures. However, we could not conclude that the agreement between calculated and observed results is satisfactory. In particular, the $q_T = 1/3$ subphase with three layer periodicity, which is experimentally most stable, is never stabilized in the above calculated results. This means that an essential factor is missing. It must be the additional polarization produced by the 'discrete' flexoelectric effect, which was originally introduced in order to explain the non-planar structures of the subphase [32]. In Sm$C^*$ and Sm$C_A^*$, we could not detect the discrete flexoelectric effect. In the subphases, the dominant ordering forces stabilizing Sm$C^*$ and Sm$C_A^*$, respectively, are nearly equal, and hence the otherwise non-detectable discrete flexoelectric effect must become to play an essential role. The resulting discrete flexoelectric polarization can be written, in the first approximation, in the form of

$$P_{f,i} = \frac{\mu_f \chi_{\perp}}{2D}[\mathbf{e} \times (\mathbf{w}_{i+1} - \mathbf{w}_{i-1}], \tag{12}$$

where $\mathbf{w}_{i\pm1} = (\mathbf{e} \cdot \mathbf{n}_{i\pm1})[\mathbf{e} \times \mathbf{n}_{i\pm1}]$ are the order parameters of the neighboring layers '$i \pm 1$', respectively, and D = L cos $\Theta$ is the thickness of the smectic layer, $\mu_f$ the 'flexoelectric coefficient', and $\chi_{\perp}$ is the susceptibility. Figure 7 illustrates how the discrete flexoelectric polarization $P_{f,i}$, together with the ordinary one $P_{o,i}$, emerges in the Ising model of the $q_T = 1/3$ subphase. Note that $P_{f,i}$, is in the tilt plane and that $S_i$ takes not only $\pm 1$ but also 0. Thus Eq. (11) also allows us to calculate the relative stability of a particular subphase specified by $q_T$ using the Casimir type long-range interaction due to the $P_{f,i}$ fluctuations. some numerically calculated results are shown in Figure 8, which forms a striking contrast to Figure 6 in the sense that the $q_T = 1/3$ subphase exclusively stabilized. What this means is, we believe, that not only the considerably non-planar structure of the observed $q_T = 1/3$ subphase but also the stable emergence in itself is the manifestation of an important role played by the discrete flexoelectric effect. Furthermore, the presence of $P_{f,i}$ justifies the treatment of this paper in spite of the previous experimental finding that Sm$C_{\alpha}^*$ emerges even when $P_{o,i}$ is zero in a mixture [40][1]; there is no inevitability that both $P_{o,i}$ and $P_{f,i}$ become zero at the same mixing ratio.

[1]We once considered that the mechanism of SM$C_{\alpha}^*$ emergence was slightly different from that of the other subphases and that the Casimir type long-range interaction due to polarization fluctuations did not mainly cause Sm$C_{\alpha}^*$.

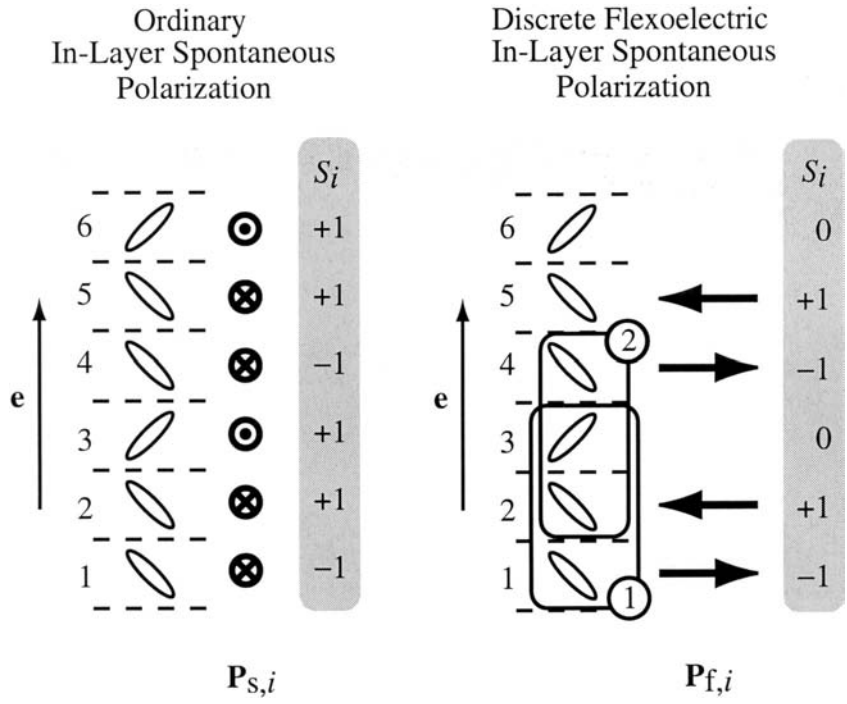


**FIGURE 7** In-layer spontaneous polarizations. The ordinary and 'discrete flexoelectric' in-layer spontaneous polarizations, $P_{o,i}$ and $P_{f,i}$, were obtained in terms of the Ising model. Note that $P_{f,i}$ appears in the tilt plane and has $S_i = \pm 1$ or 0 although $P_{o,i}$ is perpendicular to it and has $S_i = \pm 1$.

## 4. OPEN QUESTIONS RAISED

In the actual cases, both of the polarizations, $P_{o,i}$ and $P_{f,i}$, must contribute to the subphase emergence. To see their cooperative contributions very roughly, we replaced Eq. (9) by the simple addition of both contributions,

$$\tilde{J}_o \tilde{T} \sum_i \sum_j \frac{S_i S_j}{|i-j|^2} + \tilde{J}_f \tilde{T} \sum_i \sum_j \frac{S_i S_j}{|i-j|^2}, \tag{13}$$

and obtained Figure 9. The parameters were tentatively chosen as $\tilde{\mathcal{J}}_o / \tilde{v}_{eff}^{\parallel} = 0.5 \times 10^{-4}$ and $\tilde{\mathcal{J}}_f / \tilde{v}_{eff}^{\parallel} = 1.0 \times 10^{-4}$, which refer to the contributions from the ordinary and discrete flexoelectric polarizations,

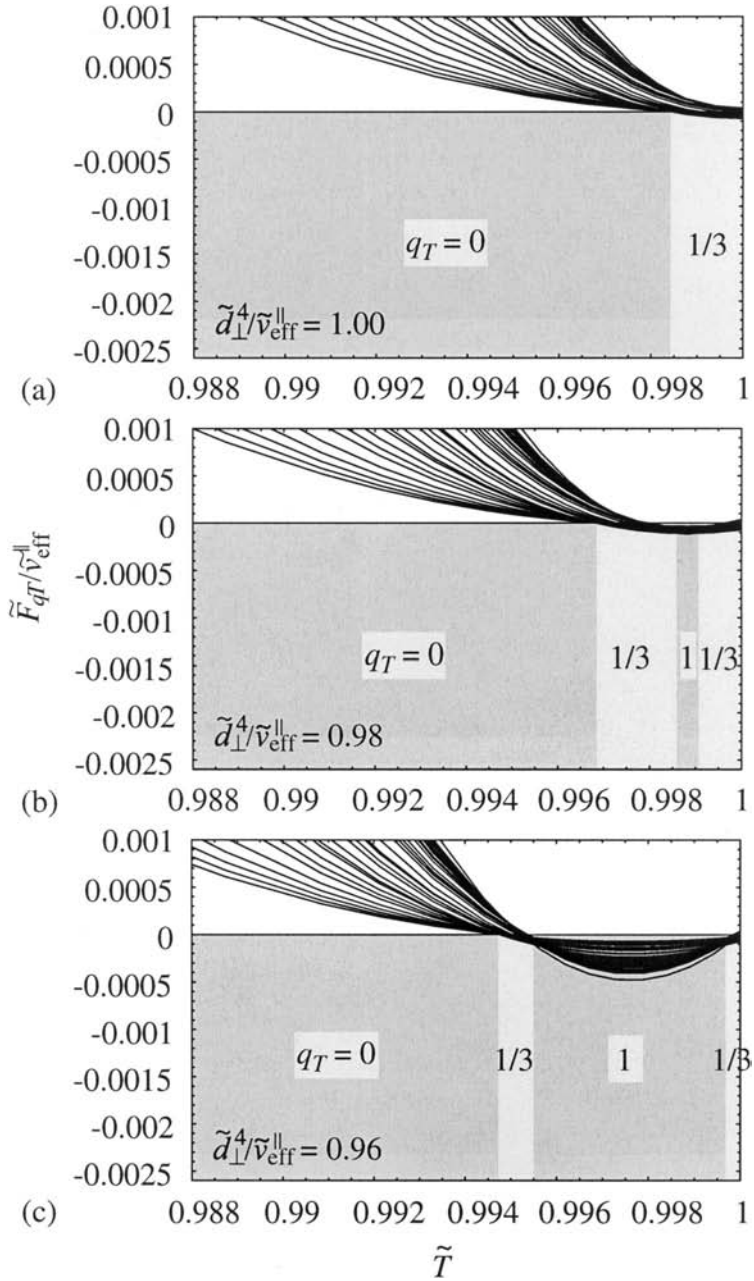


**FIGURE 8** Subphase emergence due to discrete flexoelectric polarization. The degeneracy lifting near the frustration points was calculated by taking account of the Casimir type long-range interaction due to the discrete flexoelectric polarization $P_{f,i}$. Note that the $q_T = 1/3$ subphase is exclusively stabilized. Parameters used are $\alpha/B = 5$ and $\tilde{d}_\perp^4/\tilde{v}_{eff}^{\parallel} = 1.0$ in (a), 0.98 in (b), and 0.96 in (c).

respectively. The subphase sequence between Sm$C_A^*$ and Sm$C^*$ shown in Figure 9 (b) is quite similar to the actually observed one; both of the $q_T = 1/3$ and 1/2 subphases stably exist and three additional ones appear to emerge. Such is the case with the calculated results, but the simple addition used is apparently inappropriate. As explained in Figure 7, $P_{f,i}$ is in the tilt plane, while $P_{o,i}$ is perpendicular to it. The first open question raised is how to generalize Eq. (8) so that we can calculate the Casimir type long-range interaction due to the fluctuations of polarizations that may not be parallel one another. After attaining this generalization, we will be able to reproduce more faithfully a variety of subphase sequences actually observed in compounds and mixtures. At the same time, we will be able to show the stabilization of the non-planar subphase structures by using such generalized Eq. (8) together with Eq. (6).

The second question is concerned with the tilt angle dependence of the Frank elastic constants. We assumed $\sqrt{K_\parallel K_\perp} \propto \sin^2 \Theta$ in deriving Eq. (9); hence Eq. (9) does become independent of $\Theta$, resulting in the degeneracy lifting even at $\tilde{T} = 1$ as seen in all the calculated results given in Figures 6, 8 and 9. When the tilt angle becomes zero at $\tilde{T} = 1$, all the subphases should have the same free energy and Eq. (8) should be zero there. Consequently, the aforementioned degeneracy lifting at $\tilde{T} = 1$ is inappropriate and considerably influences the calculated relative subphase stability and makes worse the agreement between observed and calculated results shown in Figures 1 and 9 (c). Note that, as pointed out in Introduction, Sm$C_\alpha^*$ is antiferroelectric in the high temperature region just below Sm$A$ and gradually becomes ferrielectric with decreasing temperature at least in two compounds, MHPOBC and MHPOCBC [5,8]. The calculated results shown in Figures 6 and 8 appear to be favorable to some extent in reproducing this experimentally observed tendency, if we choose the tilt angle dependence of $\sqrt{K_\parallel K_\perp}$ appropriately. Since Sm$C_\alpha^*$ is quite uniaxial as notice experimentally, in other words, it may have the short-pitch helical structure, the high and low temperature antiferroelectric and ferrielectric regions must be principally described by the $q_T = 1/2$ and 1/3 structures in our scenario. Because of the Casimir type long-range interaction due to the fluctuations of the polarizations, of the flexoelectric polarization, in particular, the stable configurations of these $q_T = 1/2$ and 1/3 structures may become much more deviated from the Ising (planar) structures than those observed in the subphases emerging between Sm$C_A^*$ and Sm$C^*$ and hence look like uniaxial. Note that the $q_T = 0$ structure of Sm$C_A^*$ could not be non-planar since the discrete flexoelectric polarization is not produced when the short-range interaction explicitly stabilizes the anticlinic structure as explained in Section 3. In Sm$C_\alpha^*$, however, the very small tilt angle and hence the large thermal fluctuations must promote the stabilization of its non-planar structure and even the $q_T = 0$ structure just below Sm$A$ as

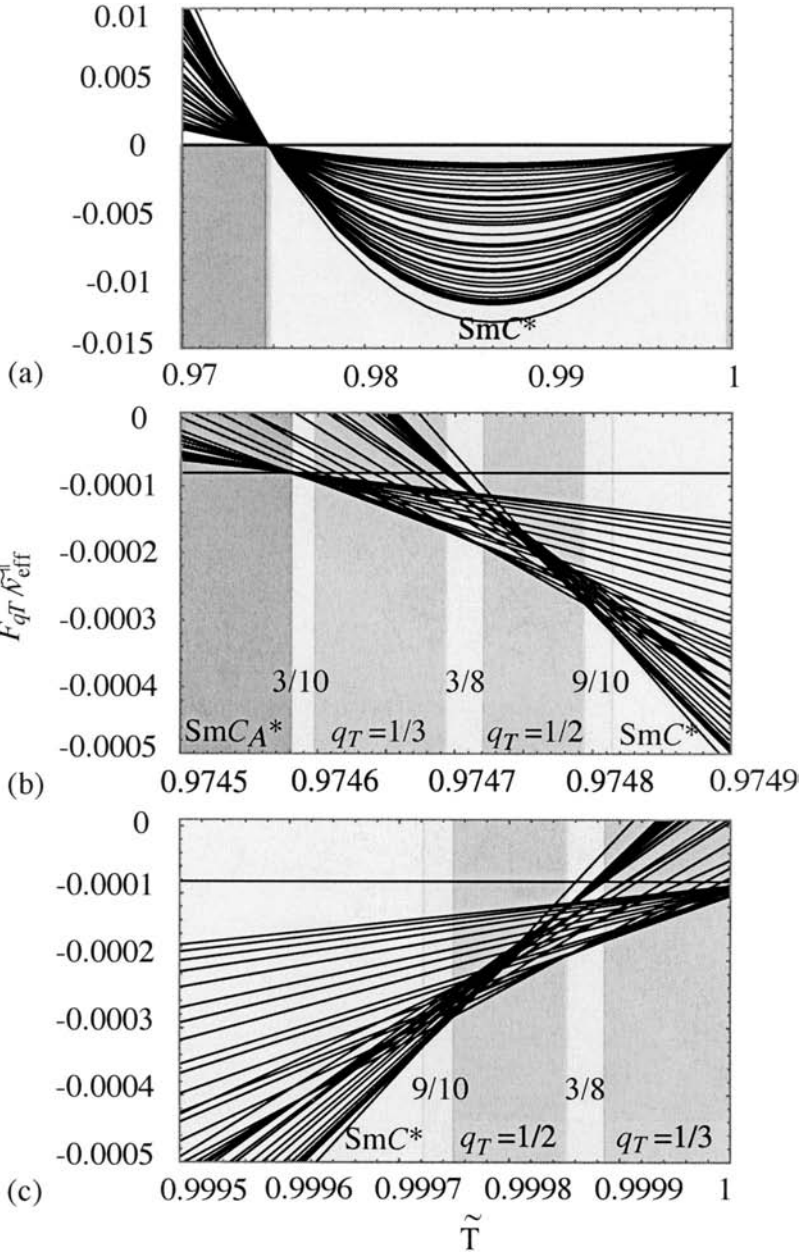

seen in Figure 6 may become uniaxial. Likewise, the transitions within Sm$C^*_\alpha$, *e.g.* between antiferroelectric $q_T = 1/2$ and ferrielectric $q_T = 1/3$, may become indistinct.

The third and final open question is the experimental clarification of the detailed subphase structures other than $q_T = 1/3$ (Sm$C^*_\gamma$) and $q_T = 1/2$ (AF). Some of the promising materials are: 12BIMF10 for the subphase between Sm$C^*_A$ and $q_T = 1/3$ (Sm$C^*_\gamma$), and MHFPDBC for the subphase between $q_T = 1/2$ (AF) and Sm$C^*$ [41]. Particularly interesting is the MHPBC-TFMHPBC mixture systems for studying Sm$C^*_\alpha$ [10]. Apparently there exist several types of sequences:

(1) Sm$C^*_\alpha$ as well as the other series of subphases emerge on both high and low temperature sides of Sm$C^*$;
(2) Sm$C^*$ disappears and Sm$C^*_\alpha$ emerges just above another subphase, *e.g.* $q_T = 1/3$ (Sm$C^*_\gamma$) or $q_T = 1/2$ (AF);
(3) Sm$C^*_\alpha$ alone emerges directly above Sm$C^*_A$;
(4) Sm$C^*_\alpha$ alone emerges directly above Sm$C^*$;
(5) Sm$C^*_\alpha$ does not emerge but the other series of subphases exists below Sm$C^*$.

Systematic investigations in a variety of materials using sophisticated techniques will confirm the validity of the scenario described in this paper in terms of the two kinds of fluctuation forces; one is the interlayer orientational correlation between transverse molecular dipoles and the other is the Casimir type long-range interaction due to the fluctuations of not only the ordinary but also the 'discrete flexoelectric' in-layer spontaneous polarizations. Experimental results should be analyzed very carefully, since contradictory conclusions were derived in a variety of compounds by using several different techniques [42–60].

**FIGURE 9** Subphase emergence due to both $P_{o,i}$ and $P_{f,i}$. The degeneracy lifting was calculated by simply adding both $P_{o,i}$ and $P_{f,i}$ effects. Parameters used are $\alpha/B = 5$, $\tilde{d}^4_\perp/\tilde{v}^\parallel_{eff} = 0.8$, $\tilde{\mathcal{J}}_o/\tilde{v}^\parallel_{eff} = 0.5 \times 10^{-4}$ and $\tilde{\mathcal{J}}_f/\tilde{v}^\parallel_{eff} = 1.0 \times 10^{-4}$. The subphase sequence between Sm$C^*_A$ and Sm$C^*$ given in (b) is quite similar to the actually observed one, although the simple addition used is apparently inappropriate. On the other hand, the staircase character of Sm$C^*_\alpha$ given in (c) does not reproduce the experimentally observed tendency: antiferroelectric at high temperature just below Sm$A$ and ferrielectric at low temperatures just above Sm$C^*$ or Sm$C^*_A$ [5,8]. The main reason for this discrepancy is due to the inappropriate assumption of $\sqrt{K_\parallel K_\perp} \propto \sin^2\Theta$ and the resulting degeneracy lifting even at $\tilde{T} = 1$ where $\Theta = 0$.

## REFERENCES


[1] Meyer, R. B., Liebert, L., Strzelecki, L., & Keller, P. (1975). *J. Phys. (Paris)*, *36*, L69.
[2] Meyer, R. B. (1977). *Mol. Cryst. Liq. Cryst. 40*, 33.
[3] Chandani, A. D. L., Gorecka, E., Ouchi, Y., Takezoe, H., & Fukuda, A. (1989). *Jpn. J. Appl. Phys.*, *28*, L1265.
[4] Orihara, H. & Ishibashi, Y. (1990). *Jpn. J. Appl. Phys.*, *29*, L115.
[5] Fukuda, A., Takanishi, Y., Isosaki, T., Ishikawa, K., & Takezoe, H. (1994). *J. Mater. Chem.*, *4*, 997.
[6] Fukui, M., Orihara, H., Yamada, Y., Yamamoto, N., & Ishibashi, Y. (1989). *Jpn. J. Appl. Phys.*, *28*, L849.
[7] Isozaki, T., Fujikawa, T., Takezoe, H., Fukuda, A., Hagiwara, T., Suzuki, Y., & Kawamura, I. (1992). *Jpn. J. Appl. Phys.*, *31*, L1435.
[8] Takanishi, Y., Hiraoka, K., Agrawal, V. K., Takezoe, H., Fukuda, A., & Matsushita, M. (1991). *Jpn. J. Appl. Phys.*, *30*, 2023.
[9] Hiraoka, K., Takanishi, Y., Skarp, K., Takezoe, H., & Fukuda, A. (1991). *Jpn. J. Appl. Phys.*, *30*, L1819.
[10] Isozaki, T., Ishikawa, K., Takezoe, H., & Fukuda, A. (1993). *Ferroelectrics*, *147*, 121.
[11] Isozaki, T., Takezoe, H., Fukuda, A., Suzuki, Y., & Kawamura, I. (1994). *J. Mater. Chem.*, *4*, 237.
[12] Mach, P., Pindak, R., Levelut, A.-M., Barois, P., Nguyen, H. T., Huang, C. C., & Furenlid , L. (1998). *Phys. Rev. Lett.*, *81*, 1015.
[13] Levelut, A.-M. & Pansu, B. (1999). *Phys. Rev. E*, *60*, 6803.
[14] Johnson, P. M., Olson, D. A., Pankratz, S., Nguyen, H. T., Goodby, J. W., Hird, M., & Huang, C. C. (2000). *Phys. Rev. Lett.*, *84*, 4870.
[15] Johnson, P. M., Pankrats, S., Mach, P., Nguyen, H. T., & Huang, C. C. (1999). *Phys. Rev. Lett.*, *83*, 4073.
[16] Schlauf, D., Bahr, Ch., & Nguyen, H. T. (1999). *Phys. Rev. E*, *60*, 6816.
[17] Olson, D. A., Pankratz, S., Johnson, P. M., Cady, A., Nguyen, H. T., & Huang, C. C. (2001). *Phys. Rev. E*, *63*, 061711.
[18] Laux, V., Isaert, N., Nguyen, H. T., Cluzeau, P., & Destrade, C. (1996). *Ferroelectrics*, *179*, 25.
[19] Laux, V., Isaert, N., Joly, G., & Nguyen, H. T. (1999). *Liq. Cryst.*, *26*, 361.
[20] Akizuki, T., Miyachi, K., Takanishi, Y., Ishikawa, K., Takezoe, H., & Fukuda, A. (1999). *Jpn. J. Appl. Phys.*, *38*, 4832.
[21] Dolganov, P. V., Suzuki, Y., & Fukuda, A. (2002). *Phys. Rev. E*, *65*, 031702.
[22] Sun, H., Orihara, H., & Ishibashi, Y. (1993). *J. Phys. Soc. Jpn.*, *62*, 2706.
[23] Roy, A. & Madhusudana, N. V. (1998). *Europhy. Lett.*, *41*, 501.
[24] Cepic, M., & Zeks, B. (2001). *Phys. Rev. Lett.*, *87*, 085501.
[25] Yamashita, M. & Miyazima, S. (1993). *Ferroelectrics*, *148*, 1.
[26] Matsumoto, T., Fukuda, A., Johno, M., Motoyama, Y., Yui, T., Seomun, S. S., & Yamashita, M. (1999). *J. Mater. Chem.*, *9*, 2051.
[27] Takeuchi, M., Chao, K., Ando, T., Matsumoto, T., Fukuda, A., & Yamashita, M. (2000). *Ferroelectrics*, *246*, 1.
[28] Koda, T. & Kimura, H. (1996). *J. Phys. Soc. Jpn.*, *65*, 2880.
[29] Nakagawa, M. (2000). *Jpn. J. Appl. Phys.*, *39*, 4068.
[30] Fisher, M. E. & Selke, W. (1980). *Phys. Rev. Lett.*, *44*, 1502.
[31] Bak, P. & von Boehm, J. (1980). *Phys. Rev. B*, *21*, 5297.
[32] Osipov, M. A., Fukuda, A., & Hakoi, H. (2002). *Mol. Cryst. Liq. Cryst.*, in press.
[33] Bak, P. (1986). *Phys. Today*, *39*, 38.
[34] Bak, P. & Bruinsma, R. (1982). *Phys. Rev. Lett.*, *49*, 249.

[35] Bruinsma, R. & Bak, P. (1983). *Phys. Rev. B*, *27*, 5824.
[36] Prost J. & Bruinsma, R. (1993). *Ferroelectrics*, *148*, 25.
[37] Bruinsma, R. & Prost J. (1994). *J. Phys. (France) II*, *4*, 1209.
[38] Young, C. Y., Pindak, R., Clark, N. A., & Meyer, R. B. (1978). *Phys. Rev. Lett.*, *40*, 773.
[39] Osipov, M. A. & Fukuda, A. (2000). *Phys. Rev. E*, *62*, 3724.
[40] Yamada, K., Takanishi, Y., Ishikawa, K., Takezoe, H., Fukuda, A., & Osipov, M. A. (1997). *Phys. Rev. E*, *56*, R43.
[41] Itoh, K., Kabe, M., Miyachi, K., Takanishi, Y., Ishikawa, K., Takezoe, H., & Fukuda, A. (1997). *J. Mater. Chem.*, *7*, 407.
[42] Hiraoka, K., Takanishi, Y., Takezoe, H., Fukuda, A., Isozaki, T., Suzuki, Y., & Kawamura, I. (1992). *Jpn. J. Appl. Phys.*, *31*, 3394.
[43] Okabe, N., Suzuki, Y., Kawamura, I., Isozaki, T., Takezoe, H., & Fukuda, A. (1992). *Jpn. J. Appl. Phys.*, *31*, L793.
[44] Isozaki, T., Hiraoka, K., Takanishi, Y., Takezoe, H., Fukuda, A., Suzuki, Y., & Kawamura, I. (1992). *Liq. Cryst.*, *12*, 59.
[45] Isozaki, T., Fujikawa, T., Takezoe, H., Fukuda, A., Hagiwara, T., Suzuki, Y., & Kawamura, I. (1993). *Phys. Rev. B*, *48*, 13439.
[46] Hatano, J., Hanakai, Y., Furue, H., Uehara, H., Saito, S., & Murashio, K. (1994). *Jpn. J. Appl. Phys.*, *33*, 5498.
[47] Moritake, H., Ozaki, M., Taniguchi, H., Satoh, K., & Yoshino, K. (1994). *J. Appl. Phys.*, *33*, 5503.
[48] Nguyen, H. T., Rouillon, J. C., Cluzeau, P., Sigaud, G., Destrade, C., & Isaert, N. (1994). *Liq. Cryst.*, *17*, 571.
[49] Uehara, H., Hanakai, Y., Hatano, J., Saito, S., & Murashiro, K. (1995). *Jpn. J. Appl. Phys.*, *34*, 5424.
[50] Bahr, Ch., Fliegner, D., Booth, C. J., & Goodby, J. W. (1995). *Phys. Rev. E*, *51*, R3823.
[51] Panarin, Yu. P., Kalinovskaja, O., & Vij, J. K. (1997). *Phys. Rev. E*, *55*, 4345.
[52] Mach, P., Pindak, R., Levelut, A.-M., Barois, P., Nguyen, H. T., Baltes, H., Hird, M., Toyne, K., Seed, A., Goodby, J. W., Huang, C. C., & Furenlid, L. (1999). *Phys. Rev. E*, *60*, 6793.
[53] Beaubois, F., Marcerou, J. P., Nguyen, H. T., & Rouillon, J. C. (2000). *Eur. Phys. J. E*, *3*, 273.
[54] Bourny, V., Fajar, A., & Orihara, H. (2000). *Phys. Rev. E*, *62*, R5903.
[55] Sigarev, A. A., Vij, J. K., Panarin, Yu., & Goodby, J. W. (2000). *Phys. Rev. E*, *62*, 2269.
[56] Shtykov, N. M., Vij, J. K., Lewis, R. A., Hird, M., & Goodby, J. W. (2000). *Phys. Rev. E*, *62*, 2279.
[57] Bourny, V. & Orihara, H. (2001). *Phys. Rev. E*, *63*, 021703.
[58] Shtykov, N. M., Vij, J. K., & Nguyen, H. T. (2001). *Phys. Rev. E*, *63*, 051708.
[59] Matkin, L. S., Watson, S. J., Gleeson, H. F., Pindak, R., Pitney, J., Johnson, P. M., Huang, C. C., Barois, P., Levelut, A.-M., Srajer, G., Pollman, J., Goodby, J. W., & Hird, M. (2001). *Phys. Rev. E*, *64*, 021705.
[60] Cady, A., Pitney, J. A., Pindak, R., Matkin, L. S., Watson, S. J., Gleeson, H. F., Cluzeau, P., Barois, P., Levelut, A.-M., Caliebe, W., Goodby, J. W., Hird, M., & Huang C. C. (2001). *Phys. Rev. E*, *64*, 050702(R).